Design and Microfabrication of a Miniature Fiber Optic Probe with Integrated Lenses and Mirrors for Raman and Fluorescence Measurements

Thitaphat Ngernsutivorakul[a,‡], **Cynthia M. Cipolla**[a,‡], **Colleen E. Dugan**[a], **Shi Jin**[a], **Michael D. Morris**[a], **Robert T. Kennedy**[a,b,*], and **Francis W. L. Esmonde-White**[a,c]

[a]Department of Chemistry, University of Michigan, 930 N. University Ave, Ann Arbor, Michigan 48109, USA

[b]Department of Pharmacology, University of Michigan, 1150 W. Medical Center Drive, Ann Arbor, Mlichigan 48109, USA

Abstract

Fiber optics coupled to components such as lenses and mirrors have seen extensive use as probes for Raman and fluorescence measurements. Probes can be placed directly on or into a sample to allow for simplified and remote application of these optical techniques. The size and complexity of such probes however limits their application. We have used microfabrication in polydimethylsiloxane (PDMS) to create compact probes that are 0.5 mm thick by 1 mm wide. The miniature probes incorporate pre-aligned mirrors, lenses, and two fiber optic guides to allow separate input and output optical paths suitable for Raman and fluorescence spectroscopy measurements. The fabricated probe has 70% unidirectional optical throughput and generates no spectral artifacts in the wavelength range of 200 to 800 nm. The probe is demonstrated for measurement of fluorescence within microfluidic devices and collection of Raman spectra from a pharmaceutical tablet. The fluorescence limit of detection was 6 nM when using the probe to measure resorufin inside a 150 μm inner diameter glass capillary, 100 nM for resorufin in a 60 μm deep × 100 μm wide PDMS channel, and 11 nM for fluorescein in a 25 μm deep × 80 μm wide glass channel. It is demonstrated that the same probe can be used on different sample types, e.g. microfluidic chips and tablets. Compared to existing Raman and fluorescence probes, the microfabricated probes enable measurement in smaller spaces and have lower fabrication cost.
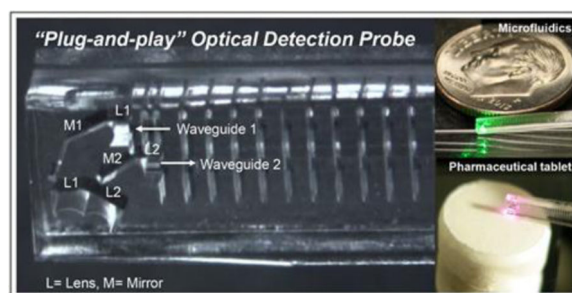
Graphical Abstract

[*]Corresponding author, rtkenn@umich.edu.

[c]Current address: Kaiser Optical Systems Inc., 371 Parkland Plaza, Ann Arbor, Michigan 48103, USA

[‡]Thitaphat Ngernsutivorakul and Cynthia M. Cipolla contributed equally to this work.

Conflict of Interest

The authors declare that they have no conflict of interest.

A microfabricated spectroscopic probe with integrated optics was developed for chemical detection in small spaces and in remote applications

Keywords

Microfabrication/microfluidics; miniaturized optical probe; spectroscopy; remote application; diagnostics

Introduction

Raman and fluorescence spectroscopies, are powerful analytical tools due to their high sensitivity, fast response, and information content. One format for these techniques is based on fiber optic probes that incorporate lenses and mirrors on the probe tip for guiding light between sample and optical fibers. Probes can be placed directly on or into a sample providing convenient, sensor-like operation. Such probes have been used for pharmaceutical process monitoring [1], on-site environmental analysis [2, 3], study of animal tissues in vivo [4, 5] and diagnosis during clinical endoscopy [6, 7]. Although popular, the bulk of such systems can limit their application where miniaturization is needed. One area where miniaturized probes may be used is in biomedical Raman because the small size is useful in reducing invasiveness of clinical procedures and allowing measurements on smaller structures. Miniaturized probes could also enable measurements in other small environments, e.g. in microfluidic analytical systems.

Miniaturized Raman probes have been made by assembly of compact optical components (e.g., lenses and filters) and fiber optics [8, 9]. Such probes are commercially available, but they are typically expensive because of costs associated with material handling and precise optical alignment at small scale. These approaches also limit the extent of miniaturization. Commercially-available Raman probes are typically 10 mm diameter or larger. Several miniaturized fiber optic probes with lenses have been reported that are 2 mm diameter [10–12]. The smallest lensed probes reported are 0.75 mm diameter but require a complex and tedious fabrication process including assembly and alignment of a bundle of 125 μm diameter optical fibers, use of adhesives for bonding, and procedures for handling, grinding, and polishing micro-optical components [13]. For biomedical applications, sterilization protocols add mechanical requirements and manufacturing complexity. Routes to simpler fabrication and further miniaturization are of interest.

Microfabrication has emerged as a useful approach for miniaturizing optical systems [14–19]. Microfabricated optics for chemical analysis have primarily been used in microfluidic chips. Through microfabrication, optics can be integrated into a microfluidic chip with precise alignment and produced en masse. The integrated devices have been used for a variety of applications including protein separation, DNA analysis, and flow cytometry [20–22]. Many designs utilize rapid prototyping in polydimethylsiloxane (PDMS) due to advantages such as low-cost and ease of fabrication [23, 24]. Optical elements such as lenses and other waveguides can be fabricated using air-PDMS [25–30] or liquid-liquid interfaces [19, 31–37]. Typical designs use fiber optics to deliver light from the source and to collect signal from microfluidic channels [38–43]. These systems are usually developed with extensive integration in mind and their sophisticated designs allow specific performance to be achieved; however, they also require fixed optics and therefore are not flexible in their use. In addition, the optics and the microfluidic systems must be manufactured simultaneously, leading to more potential points of failure and complication in fabrication processes [44]. Although extensive precedence exists for microfabricated optical systems, little work has been reported on microfabricated free-standing probes. Such an approach may allow miniaturization of probes to enable Raman or fluorescence measurements in small spaces while also reducing the cost.

We report microfabrication of miniaturized, freestanding optical probes that can be coupled to fiber optics for Raman or fluorescence measurements. The probes are over 100-fold smaller than conventional Raman probes and are the thinnest lensed probes reported [10, 11, 13]. The miniaturized probes allow measurements in small spaces, e.g. on microfluidic devices. Finally, the potentially low cost of fabrication suggests the possibility of disposable probes that would facilitate at patient or in vivo diagnostics and other applications.

Experimental

Refractive Index (RI) Characterization and Optical Design

The RI of PDMS (Sylgard 184, Dow Corning, Midland, MI) from 200 to 800 nm was measured on a flat surface of the polymer using an ellipsometer (Sopra GESP-5, Semilab, North Billerica, MA). For these measurements, a 1/4" thick slab of PDMS was cast against a glass plate and cured between 90 °C and 100 °C for 45 min according to the manufacturer directions (1:10 ratio of parts A:B).

Zemax (Zemax LLC, Kirkland, WA) was used in non-sequential mode to model multimode glass optical fibers and air-gap optical elements in a PDMS device. The measured RI values of the PDMS were used to design lensed probes for collecting light from a liquid sample outside the PDMS probe through 0.22 numerical aperture (NA) low-OH multimode optical fibers. Mirror elements were created using total internal reflection by designing the angle of incidence on the mirror elements to be greater than the critical angle. Molds forming the optics were designed to avoid high aspect ratio elements that would resist demolding of the final device. Lens and mirror properties (position, angle, height, thickness and curvature) were adjusted to maximize fluence arriving at the focal region of the probe. For simplicity, both the excitation and collection fibers were treated as fiber optic light sources in the model. An example of Zemax simulation is shown in Fig. 1a.

Mask Design

AutoCAD was used to design lithographic masks based on the optimized Zemax models. Additional features were incorporated such as skid-and-post structures for holding the fiber optics, a bounding box to act as the outer edge of the probe mold, and registration patterns for allowing spatial alignment of multiple feature layers. Three separate layers were designed and printed onto emulsion film masks with a 7 μm minimum feature size (Fineline Imaging, Colorado Spring, CO). These masks (Fig. S1 in the Electronic Supplementary Material, ESM) were used to sequentially expose each physical layer in the lithography process. An illustration of the fiber encapsulation features are shown in Fig. 1b, which shows skids made in the first lithographic layer, posts in the second lithographic layer, and the bounding box formed in the third lithographic layer, along with a fiber snapped into place after development of the unexposed SU8.

SU-8 master mold fabrication

The master mold was microfabricated using SU-8 2075 photoresist (MicroChem, Newton, MA) on a 4-inch Si wafer (ID: 1116, University Wafer, Boston, MA). This mold consisted of 3 layers (see Fig. 1b). The first layer was created by spin-coating a 110 μm thick layer of photoresist onto the wafer, followed by a soft-bake process. The wafer was aligned to the photomask and UV exposed for 18 s at 17 mW/cm^2. The photoresist layer was then post-exposure baked to polymerize the exposed pattern. The second and third layers of the device were created via a similar process. The second layer was 300 μm thick using an exposure time of 28 s, while the third layer was 110 μm thick with 34 s exposure time. Each subsequent exposure during the UV lithography process crosslinks all polymer in the lower layers, creating solid structures down to the silicon wafer substrate. After the final post-exposure bake, SU-8 developer solution (MicroChem) with sonication was used to dissolve unexposed photoresist. The SU-8 mold surfaces were exposed to trichloro(methyl)silane (Sigma-Aldrich, St. Louis, MO) vapor to later aid the release of PDMS from the mold. All times and temperatures used for soft-bake and post-exposure bake were according to the MicroChem SU-8 2000 processing guidelines for the cumulative thickness (see Table S1 in the ESM for specific used temperatures and times).

Probe Fabrication

A schematic summarizing the fabrication process of probe can be seen in Fig. S2 in the ESM. A pair of 2 m long segments of 105 μm core/125 μm clad/ 250 μm polyimide coated low-OH optical fiber (FG105LCA, Thorlabs, Newton, NJ) were used. A 4 cm segment at the end of each fiber was stripped to remove the polyimide, and then flat-cleaved using a wide-blade fiber scribe (F-CL1, Newport, Irvine, CA). The flat-cleaved optical fiber segments were manually positioned in the SU-8 skid-and-post mold structures so that the cleaved end of the fiber was in contact with a physical stop designed at the entrance of the optical system, as illustrated in Fig. 1b. A small volume of PDMS prepolymer (~1 mL Sylgard 184, Dow Corning, Midland, MI) was prepared in a 1:10 w/w ratio, mixed, and poured into the SU-8 molds after insertion of the optical fibers. The wafer assembly was placed in a vacuum chamber to degas the PDMS. A glass microscope slide was pressed firmly into contact with the upper surface of the SU-8 mold to control the probe thickness. The silicon wafer/SU-8

mold/PDMS/glass assembly was placed in an oven at 95 °C and allowed to cure for 45 min. The lensed fiber optic probes were removed from the mold by carefully separating the glass slide and SU-8 mold. An image of the final probe is shown in Fig. 1c. The free ends of the optical fibers were terminated with standard FC-PC connectors (F12073, Fiber Instrument Sales, Inc., Oriskany, NY) using low-fluorescence epoxy (EPO-TEK 301, Epoxy Technology, Billerica, MA).

Probe optical charaterization

The transmission efficiency and spectral throughput characteristics of the microprobe were measured and compared against a probe consisting of two bare cleaved fibers. Light transmission through both probes was measured using an optical power meter (PM100, Thorlabs, Newton, NJ) and a 543 nm 1.5 mW He-Ne laser (25-LGR-193-249, Melles Griot, Carlsbad, CA). The transmittance of a NIST calibrated white light source (Hololab Calibration Accessory, HCA, Kaiser Optical Systems, Inc., Ann Arbor, MI) was measured using a spectrometer (USB2000, Ocean Optics, Dunedin, FL) to determine the spectral throughput characteristics of each probe from 200 to 800 nm with an integration time of 1 s. Reflectance spectra using one fiber as a source and the other as a collector were conducted using a fiber optic illuminator (Fiber-Lite 3100, Dolan-Jenner Industries, Woburn, MA) as the source and the same spectrometer, using Teflon as a high reflectance standard.

Fluorescence measurement

Characterization of the fluorescence performance of the probes was preliminarily conducted using a 543 nm He-Ne laser source and USB2000 spectrometer with integration times of 0.1 s to 0.5 s. The probe was placed in contact with a droplet of 10 μM resorufin on a silver-coated glass coverslip (EMF, Ithaca, NY) to determine the response of a bulk solution. To evaluate probe performance on a microfluidic chip, the probes were aligned to a PDMS microfluidic chip consisting of 60 μm deep × 100 μm wide channels, with a 100 μm thick cover layer of PDMS.

For other microfluidic fluorescence assays, the 543 nm He-Ne green laser or the 473 nm blue laser source (473-ST DPSS laser, Sintec Optronics, The Spire, Singapore) were used with a photomultiplier tube detector (Model R1547, Hamamatsu, Japan), coupled to a 580 nm (XF3022, Omega Optical, Brattleboro, VT) or a 535 nm emission filter (HQ535/50M, Chroma Technology Corp, Rockingham, VT). The voltage and amplifier gain of the PMT were set at 0.75 kV and 10^7 V/A, respectively. Initial data were collected with resorufin standards pumped through a fused silica capillary with 150 μm inner diameter × 360 μm outer diameter (Polymicro Technologies, Phoenix, AZ) and a 60 μm deep × 100 μm wide PDMS microfluidic chip. These data were used to determine the detection limit using a 249 point (~1 s) boxcar smoothing.

Fig. 2 illustrates the arrangement of the probe for on chip fluorescence detection. The PDMS microfluidic chip was fabricated by soft lithography with a channel network design used for enzyme assay and similar to a previously published device [45]. Glycerol standard solutions (Sigma-Aldrich, St. Louis, MO) were diluted to concentrations of 14, 28, 56, and 112 μM with Hank's Balanced Salt Solution (Life Technologies, Carlsbad, CA) before on-chip

mixing with free glycerol reagent (Sigma-Aldrich, St. Louis, MO) and 1 mM Amplex UltraRed (Life Technologies, Carlsbad, CA) in 35% DMSO. The solutions were pumped at 1 μL/min using a syringe pump (Chemyx, Stafford, TX). The channel was designed with serpentine mixing and incubation regions. The proprietary fluorescent product (similar to resorufin) was detected at the outlet by a microfabricated probe positioned on the chip.

The same probe was used for on-chip fluorescence detection in glass-based microfluidic devices. Borofloat glass microfluidic devices were fabricated and conditioned as previously described [46–48]. An initial experiment was conducted by passing fluorescein standards through a 25 μm deep × 80 μm wide channel. For an electrophoresis experiment, the channels were filled with sieving media (an entangled polymer solution of proprietary composition, Ab Sciex, part 390953, Framingham, MA). FITC protein ladder (LC5928, Invitrogen, Carlsbad, CA) was diluted 1:10 in the sieving media to a final concentration of ~0.1 mg/mL for each protein. The pinched injection method was used to introduce the sample in separation channel [48]. Size-based separation (separation field of 400 V/cm) was recorded 4 cm downstream from the injection cross using the probe detection system. At detection, the channel size was 15 μm deep × 50 μm wide.

For on-chip detection using the microfabricated probe, a stereotaxic frame (Model 900, KOPF, Tujunga, CA) was employed to manipulate the probe and align it to the detection zone. An analog-to-digital converter (NI USB-6008, National Instruments, Austin, TX) was used for data acquisition and collection at 250 samples/s under control of LabVIEW (Version 10.0.1, National Instruments). Data was processed in MATLAB (R2012b, MathWorks, Natick, MA).

Raman measurement

The efficacy of the probe for Raman experiments was demonstrated by collecting Raman spectra from water, DMSO, and a commercial aspirin tablet. A fiber-optic coupled Raman spectroscopy system (RamanRxn-1, Kaiser Optical Systems, Inc.) with a back-thinned deep-depletion imaging detector (Newton DU920P-BR-DD, ANDOR Technology, Belfast, Ireland) was operated in full-vertical-binning mode to collect Raman spectra. A 100 mW, 785 nm excitation laser was connected to the 65° incidence fiber, while the Raman signal was collected through the 90° incidence fiber channel. Raman spectra were collected with 5 s acquisition times.

Results and Discussion

Design and Fabrication of the Probes

Our goal was to design a free-standing probe with integrated optics that could focus and collect light from outside the probe, be easily coupled to fiber optics, and have separate input (e.g. excitation) and output (e.g. emission) paths. Fig. 1 illustrates the side-firing design that was fabricated and tested. The probe contains guides for inserting optical fibers precisely and optics at the probe tip for guiding light in and out of the probe.

One consideration for precise design of optical elements is the RI of the PDMS, which can vary significantly depending on selected wavelengths, curing times, and temperatures. The

measured RI values at 200 to 800 nm wavelengths ranged from 1.42 to 1.58 for PDMS (Fig. S3 in the ESM). The RI change is particularly small between 400 and 800 nm. This small RI dispersion suggests the possibility of microfabricating PDMS lenses with low chromatic aberration at the wavelengths of visible light. On the other hand, the RI increases rapidly at the wavelengths of UV light (200 to 400 nm).

The measured RI values were used with Zemax to design optical elements that were optimized for light in the range of 200 to 800 nm (Fig. 1a). The cylindrical optics (e.g. lens and mirrors) in the fabricated probe were designed to generate a line-shaped focus 100 μm below a coverslip. In the design, one fiber optic is used for excitation while the other is for collection of emitted light. The probe generates focused light at 90° incidence for the first fiber and 65° incidence for the second fiber. Folding mirrors are incorporated so that the source and collection regions overlap as necessary for Raman or fluorescence measurements. The probe design has the benefit of maintaining the source and collection optical fibers along a common axis on a single side of the sample which facilitates having a small but robust probe. The side-firing design also avoids probe deformation during alignment to the sample.

To accommodate two 125 μm diameter optical fibers, the width of these probes must be at least 400 μm, including the protective layers. In practice, a 90° side-firing probe incorporating two 30° incidence total-internal-reflectance based mirrors requires a minimum width of approximately 1.1 mm based on the optimized Zemax model. These probes have a total thickness of approximately 500–600 μm, including an externally bonded 100 μm PDMS cover layer.

We fabricated devices using inexpensive emulsion masks with a surface roughness of approximately 2 μm. The layer thicknesses are within 2% of the design values, and the optical features are within 2% of the target size. The aspect ratio has not been well optimized; instead, feature sizes are deliberately kept large to avoid issues with mold fabrication and demolding of the PDMS structures. Resulting probes were too small and flexible to be handled conveniently; thus, a holder was required for further experiments. In this study, we selected a commercially-available stereotaxic alignment system for use as a holder and a micro-positioner. The stereotaxic system allowed us to precisely manipulate probe position and to secure probe placement on/in sample substrates.

Optical Characterization of Probes

To evaluate optical performance of the microprobe, a series of comparisons were made to a probe consisting of two cleaved bare fibers assembled side by side with identical FC connections. The optical throughput of the microfabricated probe was determined by injecting laser light at the FC fiber interface and measuring the optical power transmitted through the probe face. The bare fiber probe has 84% throughput while the probe with fabricated optics has 70% throughput. These results suggest that the majority of the 16% loss in the bare fiber is due to losses in injecting light through the FC connector, and in the microprobe an additional 14% loss is due to the probe optical elements. Reflection losses could potentially be further reduced by the use of coupling gels or index-matching fluids, which were not used in this case. To determine if any spectral artifacts are caused by the

microfabricated optics, we compared white light throughput of the microfabricated probes to the throughput of a bare fiber using a spectrometer. The spectra are identical for both probe types, as illustrated in Fig. 3a, indicating no spectral artifacts are generated by the microoptical system.

To compare the background scattering arising from the probe optics, a white light reflectance spectrum was collected with the probes pointing into free space in a dark room, as shown in Fig. 3b. The scattered white light background generated from the microfabricated probe is significant, while the bare fiber probe has no discernible background because the bare fiber probe has no interfaces which can scatter light from the excitation channel back into the collection channel. The 2 μm roughness causes elastic light scattering from the optical surfaces of the micofabricated probe. Next, the collection efficiency from a highly scattering material (Teflon) was measured. Both probe types have approximately the same collection efficiency, with slightly different spectral collection efficiency due to wavelength-dependent light scattering effects. However, when collection efficiency is tested against a transparent PDMS slab, the bare fiber probe collects 3.3 times more signal than the microprobe. This difference occurs because the surface reflections from the PDMS slab are collected very efficiently by the two parallel fibers. The spatial offset between the excitation and collection paths in the microprobe allow little reflectance to be collected, with half of this reflectance arising within the microprobe as shown by the reflectance in air.

When measuring fluorescence of resorufin in bulk solution, the bare fiber probe collects 2.2 fold more fluorescence than the microfabricated probe because of a higher overall collection solid angle (Fig. 3c). However, when measuring resorufin in a channel buried 100 μm below the surface of the PDMS microfluidic device, the microfabricated probes detect fluorescence comparable to that of bulk solution, whereas the bare fiber probe returned no discernible fluorescence. This result is because the lensed microprobe focuses the light below the surface and into the channel. The bare fiber probe collects the excitation laser light reflected from the PDMS microchip so that the laser signal overwhelms any fluorescence (Fig. 3d). The much higher reflectance from the PDMS surface when using the bare probe is in agreement with the results shown in Fig. 3b, where the surface reflectance of the bare fiber probe is several fold greater than for the microprobe. The overall results indicate the utility of incorporating optics on a microprobe for collecting light from within a microfluidic sample.

Numerical aperture (NA) is used to characterize the angles accepted through an optical system. In this case, the NA of the probe was defined as a certain angular range over which the probe can deliver light to and collect light from a sample. The NA of the probes made for this study were limited by the NA of the fiber, which was 0.22.

Fluorescence Detection in Microfluidic Systems

Fluorescence in microfluidics or capillaries (e.g., for capillary electrophoresis detection) is usually measured using microscopes or other external assembled optics. Alternatively, microfabricated optics can be built into a chip [25, 26]. Here we evaluated the microfabricated probe to measure fluorescence within capillaries or microfluidic chips. For

these experiments, the probe was positioned over a capillary (e.g. Fig S4, see ESM) or microfluidic chip (e.g. Fig. 2) with a laser coupled to the inlet and detector to the outlet of the probe.

We initially tested the probe by detecting resorufin standards in a 150 μm inner diameter × 360 μm outer diameter fused-silica capillary. Fig. S4 in the ESM illustrates the trace detected using the probe while passing plugs of 52 nM resorufin through the capillary. Responses to a series of concentrations from 0.05 to 10 μM were linear with R^2 of 0.997. The limit of detection (LOD), determined as the concentration to give a signal 3 times the standard deviation of the blank, was 6 nM. These results demonstrate that the probe is suitable for fluorescence measurements within a capillary.

The probe was then placed on a 60 μm deep × 100 μm wide PDMS chip for on-chip measurement of 0 to 75 μM resorufin standards. This range of standard concentrations was selected to match with the concentrations of proprietary fluorescent products in the following enzyme assay. Fluorescence detection of different resorufin concentrations is shown in Fig. 4a. As shown in Fig. 4b, the fluorescence changes were linear with concentration with R^2 of 0.990. The LOD was determined to be 100 nM. Next, we evaluated the performance of the probe to act as a detector for a microfluidic chip used for fluorescence enzyme assay. The probe was positioned over a PDMS chip used for continuous flow enzyme assay of glycerol (Fig 2). The signals of the fluorescent products from different glycerol concentrations pumped through the chip are shown in Fig. 4c. Each trace represents the signals upon switching between low and high glycerol concentrations. The fluorescence assay, using the probe as an optical probe, resulted in a linear response with R^2 of 0.988, as shown in Fig. 4d. The calculated LOD was 700 nM for glycerol. With probe detection, analytical performance of the on-chip assay is comparable to our previously reported on-line enzyme assay using a fluorescence microscope for detection [49] and other commercial glycerol assay kits [50]. Thus, in this case where the LOD is determined by the enzyme assay, the probe provides comparable LODs but in a compact and low-cost probe.

The same probe was tested for fluorescence detection in glass microfluidic devices. The probe was positioned over a 25 μm deep × 80 μm wide glass microfluidic chip while pumping 0 to 100 nM fluorescein through the device. The trace in Fig. 5a illustrates the detection of fluorescent changes at different fluorescein concentrations. The resulting calibration curve was linear with R^2 of 0.999, as shown in Fig. 5b. The LOD was determined to be 11 nM. The probe was then used for detection of microchip electrophoresis separation of a fluorescent protein ladder (Fig. 5c). The probe was placed on a glass-based electrophoresis chip near the end of a 15 μm deep × 50 μm wide separation channel. The probe was able to detect the 7 separated proteins, as illustrated in Fig. 5d. Signal to noise ratio was reasonably comparable to our previously reported assay using a conventional microscope system that used an arc-lamp source and CCD camera for detection [51]. The individual proteins are present at ~0.014 mg/mL in this example. While the sensitivity is not excellent, this measurement is in a challenging environment of a narrow channel with brief signals. The sensitivity is counter-balanced by the ease of the measurement; the probe is merely placed over the channel. This result demonstrates the suitability of the probe for measurement of non-discrete samples within shallow and narrow detection zones.

These applications of the probe illustrate a simple way to couple fluorescence detection to a chip. Although it is difficult to compare to different experiments, the LODs are comparable to other microfabricated devices with integrated optics and optical fibers (see Table S2 in the ESM)[25, 37–39, 52–54]. A significant limitation of the current design is lack of optical filters in the probe tip. The LODs reported here could be improved by integrating optical filters directly onto the tips of the fibers, thus reducing fluorescence background due to light scattering that occurs along the fiber length [55–57]. Nevertheless, our probes have the advantage of focusing into small channels (down to 15 μm deep × 50 μm wide), enabling their use for a variety of applications, such as electrophoresis. Furthermore, the probes incorporate both excitation and emission fibers in parallel on the same side of the microfluidic device, which allows for simplified fabrication and requires less space for integration. Because the probes are standalone devices, they can be used for different applications on different chips by moving the probe from one device to another as a "plug-and-play" detector. As the major microfluidic design characteristic is the coverslip material and thickness, a given design is reusable. Indeed the same probes could be used for all the experiments described above. Individual probes are easy to clean (using Scotch® Magic™ Tape), autoclavable, and reusable due to properties of the materials used

Raman measurement

To demonstrate another application, the same microfabricated probe was used to acquire Raman spectra. Fig. 6a illustrates Raman spectra of bulk solvents (water and DMSO). These solvents have been reported to not swell PDMS [58]; hence, we do not observe any carryover or interference with measurement. The probe allows detection of several major bands of DMSO over the much weaker scatter of water, for example C-S symmetric stretch at 668 cm^{-1}, C-S antisymmetric stretch at 700 cm^{-1}, S=O stretch at 1042 cm^{-1}, and CH$_3$ degenerate deformation at 1420 cm^{-1}. Placing the probe directly on an aspirin tablet allowed detection of the characteristic Raman bands of acetylsalicylic acid including the symmetric aromatic ring C-C stretching vibration at 1606 cm^{-1} and C=O stretching vibration of the carboxyl group at the shoulder peak of 1622 cm^{-1} as well as several other observed bands below 1500 cm^{-1}, such as O-H bending vibration at 1296 cm^{-1} and C-H bending vibration at 1045 cm^{-1} and near 1200 cm^{-1} (Fig. 6b). The Raman fingerprints are consistent with previous reports [59–62]. High background at < 600 cm^{-1} is caused by the silica of the optical fibers. Addition of optical filters to fiber optic tips would reduce this background.

These results show that the microfabricated probes can be successfully employed as Raman probes. The overall size of microfabricated probes is comparable to the smallest reported lensed Raman probes [13]; however, the use of microfabrication simplifies the making of the probes and enables low cost, mass production, flexible probes, and disposability.

Conclusions and Future Directions

Microfabrication using soft lithography is a viable and cost-effective way to miniaturize spectroscopic probes. The microprobes described here are only slightly larger than the optical fibers on which they are molded. The microfabricated probes are thus smaller than commercial optical probes, enabling chemical measurements in tight spaces. As

demonstrated, the probes are versatile as the same probe can easily be transferred between samples.

Some modifications can further improve performance of the system and its ease of use. The probes can feasibly be coupled with thinner optical filters [38,55–57], more compact light sources [63,64] and detectors [65], and other miniature optics [56,66], resulting in more integrated, smaller, portable, low-cost analytical and diagnostic devices. Incorporation of filters in the tip would lower background and improve sensitivity. Better lithographic masks may be used as previously described to yield subwavelength optical quality surfaces [25]. Additional designs are possible. In principle other geometries could be fabricated such as reflectance on a single point, diffuse reflectance including a spatial offset, collimated transmission, diffuse transmission, and multiple-input multiple-output tomographic configurations.

With further development, a variety of further applications can be envisioned due to the size, cost, materials, and configuration of the probes. The probes may have excellent potential for biomedical endoscopy. The small probe size suggests potential for less-invasive endoscopy [67,68]. Compared to traditional endoscope probes, the devices are low cost to fabricate. The materials are compatible with autoclaving, offering a unique potential compatibility with biomedical applications requiring sterilization as compared to traditional assembled microprobes that require the use of adhesives and have materials with dissimilar thermal expansion coefficients. The probes also have more potential for pairing with microfluidic devices. Pairing a microfluidic device with the probes illustrates a simple approach for coupling fluorescence to a chip. Because the probe is mounted to the device, optics do not need to be incorporated into a chip allowing flexibility of design. The low cost and facile mounting of the probes may facilitate multipoint detection on a chip, a possibility that was previously restricted because of microscope dimensions [69,70]. On-chip alignment markers and probe holders for interfacing the probes to microfluidic devices can be customarily made using microfabrication or 3D printing could be used to facilitate positioning on microfluidics.

Supplementary Material

Refer to Web version on PubMed Central for supplementary material.

Acknowledgments

References

1. De Beer T, Burggraeve A, Fonteyne M, Saerens L, Remon JP, Vervaet C. Near infrared and Raman spectroscopy for the in-process monitoring of pharmaceutical production processes. Int J Pharm. 2011; 417(1–2):32–47. [PubMed: 21167266]

2. Blanco M, Villarroya I. NIR spectroscopy: a rapid-response analytical tool. TrAC Trends Anal Chem. 2002; 21(4):240–250.

3. Wolfbeis OS. Fiber-optic chemical sensors and biosensors. Anal Chem. 2008; 80(12):4269–4283. [PubMed: 18462008]

4. Wang J, Bergholt MS, Zheng W, Huang Z. Development of a beveled fiber-optic confocal Raman probe for enhancing in vivo epithelial tissue Raman measurements at endoscopy. Opt Lett. 2013; 38(13):2321. [PubMed: 23811915]

5. Schwarz RA, Arifler D, Chang SK, Pavlova I, Hussain IA, Mack V, et al. Ball lens coupled fiber-optic probe for depth-resolved spectroscopy of epithelial tissue. Opt Lett. 2005; 30(10):1159–1161. [PubMed: 15945140]

6. Shim MG, Song L-MWK, Marcon NE, Wilson BC. In vivo near-infrared Raman spectroscopy: demonstration of feasibility during clinical gastrointestinal endoscopy. Photochem Photobiol. 2000; 72(1):146–150. [PubMed: 10911740]

7. Bergholt MS, Zheng W, Ho KY, Teh M, Yeoh KG, So JBY, et al. Fiber-optic Raman spectroscopy probes gastric carcinogenesis in vivo at endoscopy. J Biophotonics. 2013 Jan 6.(1):49–59. [PubMed: 23288709]

8. Krogmeier JR, Schaefer I, Seward G, Yantz GR, Larson JW. An integrated optics microfluidic device for detecting single DNA molecules. Lab Chip. 2007; 7(12):1767. [PubMed: 18030399]

9. Kaigala GV, Bercovici M, Behnam M, Elliott D, Santiago JG, Backhouse CJ. Miniaturized system for isotachophoresis assays. Lab Chip. 2010; 10(17):2242. [PubMed: 20571691]

10. Day JCC, Bennett R, Smith B, Kendall C, Hutchings J, Meaden GM, et al. A miniature confocal Raman probe for endoscopic use. Phys Med Biol. 2009; 54(23):7077–7087. [PubMed: 19904034]

11. Grimbergen MCM, van Swol CFP, Draga ROP, van Diest P, Verdaasdonk RM, Stone N, Bosch JHLR. Bladder cancer diagnosis during cystoscopy using Raman spectroscopy. SPIE. 2009:716114–716116.

12. Latka, I.; Dochow, S.; Krafft, C.; Dietzek, B.; Bartelt, H.; Popp, J. Development of a fiber-based Raman probe for clinical diagnostics. In: Ramanujam, N.; Jürgen, P., editors. Clinical and Biomedical Spectroscopy and Imaging II. Munich, Germany: SPIE and Optical Society of America; 2011. 80872D-1-8

13. Komachi Y, Katagiri T, Sato H, Tashiro H. Improvement and analysis of a micro Raman probe. Appl Opt. 2009; 48(9):1683–1696. [PubMed: 19305466]

14. Burns MA, Johnson BN, Brahmasandra SN, Handique K, Webster JR, Krishnan M, Sammarco TS, Man PM, Jones D, Heldsinger D. An integrated nanoliter DNA analysis device. Science. 1998; 282(5388):484–487. [PubMed: 9774277]

15. Roulet J-C, Völkel R, Herzig HP, Verpoorte E, de Rooij NF, Dändliker R. Performance of an integrated microoptical system for fluorescence detection in microfluidic systems. Anal Chem. 2002; 74(14):3400–3407. [PubMed: 12139046]

16. Verpoorte E. Focus. Lab Chip. 2003; 3(3):42N–52N.

17. Roman GT, Kennedy RT. Fully integrated microfluidic separations systems for biochemical analysis. J Chromatogr A. 2007; 1168(1):170–188. [PubMed: 17659293]

18. Mogensen KB, Kutter JP. Optical detection in microfluidic systems. Electrophoresis. 2009; 30(S1):S92–S100. [PubMed: 19517511]

19. Zeng X, Jiang H. Liquid tunable microlenses based on MEMS techniques. J Phys Appl Phys. 2013; 46(32):323001.

20. Vieillard J, Mazurczyk R, Morin C, Hannes B, Chevolot Y, Desbene P, Krawczyk S. Application of microfluidic chip with integrated optics for electrophoretic separations of proteins. J Chromatogr B. 2007; 845(2):218–225.

21. Bliss CL, McMullin JN, Backhouse CJ. Rapid fabrication of a microfluidic device with integrated optical waveguides for DNA fragment analysis. Lab Chip. 2007; 7(10):1280. [PubMed: 17896011]

22. Godin J, Chen C-H, Cho SH, Qiao W, Tsai F, Lo Y-H. Microfluidics and photonics for Bio-System-on-a-Chip: A review of advancements in technology towards a microfluidic flow cytometry chip. J Biophotonics. 2008; 1(5):355–376. [PubMed: 19343660]

23. Becker H, Gärtner C. Polymer microfabrication technologies for microfluidic systems. Anal Bioanal Chem. 2007 Nov 8; 390(1):89–111. [PubMed: 17989961]

24. Nge PN, Rogers CI, Woolley AT. Advances in Microfluidic Materials, Functions, Integration, and Applications. Chem Rev. 2013 Apr 10; 113(4):2550–2583. [PubMed: 23410114]

25. Camou S, Fujita H, Fujii T. PDMS 2D optical lens integrated with microfluidic channels: principle and characterization. Lab Chip. 2003; 3(1):40. [PubMed: 15100804]

26. Seo J, Lee LP. Disposable integrated microfluidics with self-aligned planar microlenses. Sens Actuators B Chem. 2004; 99(2–3):615–622.

27. Jiang L, Pau S. Integrated waveguide with a microfluidic channel in spiral geometry for spectroscopic applications. Appl Phys Lett. 2007; 90(11):111108–111108.

28. Watts BR, Zhang Z, Xu C-Q, Cao X, Lin M. Integration of optical components on-chip for scattering and fluorescence detection in an optofluidic device. Biomed Opt Express. 2012; 3(11): 2784–2793. [PubMed: 23162718]

29. Chang-Yen DA, Eich RK, Gale BK. A monolithic PDMS waveguide system fabricated using soft-lithography techniques. J Light Technol. 2005; 23(6):2088–2093.

30. Cai Z, Qiu W, Shao G, Wang W. A new fabrication method for all-PDMS waveguides. Sens Actuators Phys. 2013; 204:44–47.

31. Mao X, Waldeisen JR, Juluri BK, Huang TJ. Hydrodynamically tunable optofluidic cylindrical microlens. Lab Chip. 2007; 7(10):1303. [PubMed: 17896014]

32. Tang SKY, Stan CA, Whitesides GM. Dynamically reconfigurable liquid-core liquid-cladding lens in a microfluidic channel. Lab Chip. 2008; 8(3):395. [PubMed: 18305856]

33. Rosenauer M, Vellekoop MJ. 3D fluidic lens shaping—a multiconvex hydrodynamically adjustable optofluidic microlens. Lab Chip. 2009; 9(8):1040–1042. [PubMed: 19350083]

34. Rosenauer, M.; Vellekoop, MJ. An Adjustable Optofluidic Micro Lens Enhancing Single Cell Analysis Systems. InWorld Congress on Medical Physics and Biomedical Engineering, September 7–12, 2009. In: Dössel, O.; Schlegel, WC., editors. IFMBE Proceedings. Munich, Germany: Springer; 2010. p. 185-188.

35. Song C, Nguyen NT, Asundi AK, Low CLN. Tunable optofluidic aperture configured by a liquid-core/liquid-cladding structure. Opt Lett. 2011; 36(10):1767–1769. [PubMed: 21593884]

36. Chao KS, Lin MS, Yang RJ. An in-plane optofluidic microchip for focal point control. Lab Chip. 2013; 13(19):3886. [PubMed: 23918038]

37. Lin BS, Yang YC, Ho CY, Yang HY, Wang HY. A PDMS-Based Cylindrical Hybrid Lens for Enhanced Fluorescence Detection in Microfluidic Systems. Sensors. 2014; 14(2):2967–2980. [PubMed: 24531300]

38. Chabinyc ML, Chiu DT, McDonald JC, Stroock AD, Christian JF, Karger AM, et al. An integrated fluorescence detection system in poly(dimethylsiloxane) for microfluidic applications. Anal Chem. 2001; 73(18):4491–4498. [PubMed: 11575798]

39. Qi S, Liu X, Ford S, Barrows J, Thomas G, Kelly K, et al. Microfluidic devices fabricated in poly(methyl methacrylate) using hot-embossing with integrated sampling capillary and fiber optics for fluorescence detection. Lab Chip. 2002; 2(2):88. [PubMed: 15100840]

40. Wu MH, Cai H, Xu X, Urban JP, Cui ZF, Cui Z. A SU-8/PDMS hybrid microfluidic device with integrated optical fibers for online monitoring of lactate. Biomed Microdevices. 2005; 7(4):323–329. [PubMed: 16404510]

41. Mazurczyk R, Vieillard J, Bouchard A, Hannes B, Krawczyk S. A novel concept of the integrated fluorescence detection system and its application in a lab-on-a-chip microdevice. Sens Actuators B Chem. 2006; 118(1–2):11–19.

42. Irawan R, Tjin SC, Fang X, Fu CY. Integration of optical fiber light guide, fluorescence detection system, and multichannel disposable microfluidic chip. Biomed Microdevices. 2007; 9(3):413–419. [PubMed: 17473985]

43. Ashok PC, Singh GP, Rendall HA, Krauss TF, Dholakia K. Waveguide confined Raman spectroscopy for microfluidic interrogation. Lab Chip. 2011; 11(7):1262–1270. [PubMed: 21225053]

44. Sapuppo F, Schembri F, Fortuna L, Llobera A, Bucolo M. A polymeric micro-optical system for the spatial monitoring in two-phase microfluidics. Microfluid Nanofluidics. 2011; 12(1–4):165–174.

45. Dugan CE, Cawthorn WP, MacDougald OA, Kennedy RT. Multiplexed microfluidic enzyme assays for simultaneous detection of lipolysis products from adipocytes. Anal Bioanal Chem. 2014; 406(20):4851–4859. [PubMed: 24880873]

46. Roper MG, Shackman JG, Dahlgren GM, Kennedy RT. Microfluidic chip for continuous monitoring of hormone secretion from live cells using an electrophoresis-based immunoassay. Anal Chem. 2003; 75(18):4711–4717. [PubMed: 14674445]

47. Harrison DJ, Fluri K, Seiler K, Effenhauser CS, Manz A. Micromachining a miniaturized capillary electrophoresis-based chemical analysis system on a chip. Science. 1993; 261(5123):895–897. [PubMed: 17783736]

48. Jacobson SC, Hergenroder R, Moore AWJ, Ramsey JM. Precolumn reactions with electrophoretic analysis integrated on a microchip. Anal Chem. 1994; 66(23):4127–4132.

49. Clark AM, Sousa KM, Jennings C, MacDougald OA, Kennedy RT. Continuous-flow enzyme assay on a microfluidic chip for monitoring glycerol secretion from cultured adipocytes. Anal Chem. 2009; 81(6):2350–2356. [PubMed: 19231843]

50. Free Glycerol Colorimetric/Fluorometric Assay Kit. The BioVision Index of Manuals Online. BioVision Incorporated. 2014 [Accessed 24 Jan 2015] http://www.biovision.com/manuals/K630.pdf.

51. Jin S, Anderson GJ, Kennedy RT. Western blotting using microchip electrophoresis interfaced to a protein capture membrane. Anal Chem. 2013; 85(12):6073–6079. [PubMed: 23672369]

52. Miyaki K, Guo Y, Shimosaka T, Nakagama T, Nakajima H, Uchiyama K. Fabrication of an integrated PDMS microchip incorporating an LED-induced fluorescence device. Anal Bioanal Chem. 2005 Jun; 382(3):810–816. [PubMed: 15883790]

53. Li HF, Lin JM, Su RG, Uchiyama K, Hobo T. A compactly integrated laser-induced fluorescence detector for microchip electrophoresis. ELECTROPHORESIS. 2004; 25(12):1907–1915. [PubMed: 15213992]

54. Lee KS, Lee HLT, Ram RJ. Polymer waveguide backplanes for optical sensor interfaces in microfluidics. Lab Chip. 2007; 7(11):1539. [PubMed: 17960283]

55. Llobera A, Demming S, Joensson HN, Vila-Planas J, Andersson-Svahn H, Büttgenbach S. Monolithic PDMS passband filters for fluorescence detection. Lab Chip. 2010; 10(15):1987. [PubMed: 20485776]

56. Hofmann O, Wang X, Cornwell A, Beecher S, Raja A, Bradley DDC, et al. Monolithically integrated dye-doped PDMS long-pass filters for disposable on-chip fluorescence detection. Lab Chip. 2006; 6(8):981. [PubMed: 16874366]

57. Richard C, Renaudin A, Aimez V, Charette PG. An integrated hybrid interference and absorption filter for fluorescence detection in lab-on-a-chip devices. Lab Chip. 2009; 9(10):1371. [PubMed: 19417903]

58. Lee JN, Park C, Whitesides GM. Solvent compatibility of poly(dimethylsiloxane)-based microfluidic devices. Anal Chem. 2003; 75(23):6544–6554. [PubMed: 14640726]

59. Martens WN, Frost RL, Kristof J, Theo Kloprogge J. Raman spectroscopy of dimethyl sulphoxide and deuterated dimethyl sulphoxide at 298 and 77 K. J Raman Spectrosc. 2002; 33(2):84–91.

60. Horrocks WD Jr, Cotton FA. Infrared and Raman spectra and normal co-ordinate analysis of dimethyl sulfoxide and dimethyl sulfodize-d6. Spectrochim Acta. 1961; 17:134–147.

61. Wang C, Vickers TJ, Mann CK. Direct assay and shelf-life monitoring of aspirin tablets using Raman spectroscopy. J Pharm Biomed Anal. 1997; 16:87–94. [PubMed: 9447555]

62. Kontoyannis CG, Orkoula M. Quantitative non-destructive determination of salicylic acid acetate in aspirin tablets by Raman spectroscopy. Talanta. 1994; 41(11):1981–1984. [PubMed: 18966159]

63. Pagliara S, Camposeo A, Polini A, Cingolani R, Pisignano D. Electrospun light-emitting nanofibers as excitation source in microfluidic devices. Lab Chip. 2009; 9(19):2851. [PubMed: 19967124]

64. Yao B, Luo G, Wang L, Gao Y, Lei G, Ren K, Chen L, Wang Y, Hu Y, Qiu Y. A microfluidic device using a green organic light emitting diode as an integrated excitation source. Lab Chip. 2005; 5(10):1041. [PubMed: 16175258]

65. Kamei T, Paegel BM, Scherer JR, Skelley AM, Street RA, Mathies RA. Integrated Hydrogenated Amorphous Si Photodiode Detector for Microfluidic Bioanalytical Devices. Anal Chem. 2003 Oct; 75(20):5300–5305. [PubMed: 14710806]

66. Jiang L, Pau S. Integrated waveguide with a microfluidic channel in spiral geometry for spectroscopic applications. Appl Phys Lett. 2007; 90(11):111108.

67. Kendall C, Day J, Hutchings J, Smith B, Shepherd N, Barr H, Stone N. Evaluation of Raman probe for oesophageal cancer diagnostics. The Analyst. 2010; 135(12):3038. [PubMed: 20949209]

68. Morris MD, Finney WF, Rajachar RM, Kohn DH. Bone tissue ultrastructural response to elastic deformation probed by Raman spectroscopy. Faraday Discuss. 2004; 126:159. [PubMed: 14992405]

69. Dishinger JF, Reid KR, Kennedy RT. Quantitative monitoring of insulin secretion from single islets of Langerhans in parallel on a microfluidic Chip. Anal Chem. 2009; 81(8):3119–3127. [PubMed: 19364142]

70. Nunemaker, CS.; Dishinger, JF.; Dula, SB.; Wu, R.; Merrins, MJ.; Reid, KR., et al. Glucose metabolism, islet architecture, and genetic homogeneity in imprinting of $[Ca^{2+}]$ and insulin rhythms in mouse islets. In: Maedler, K., editor. PLoS ONE. Vol. 4. 2009. p. e8428

Author Manuscript

Author Manuscript

Author Manuscript

Author Manuscript
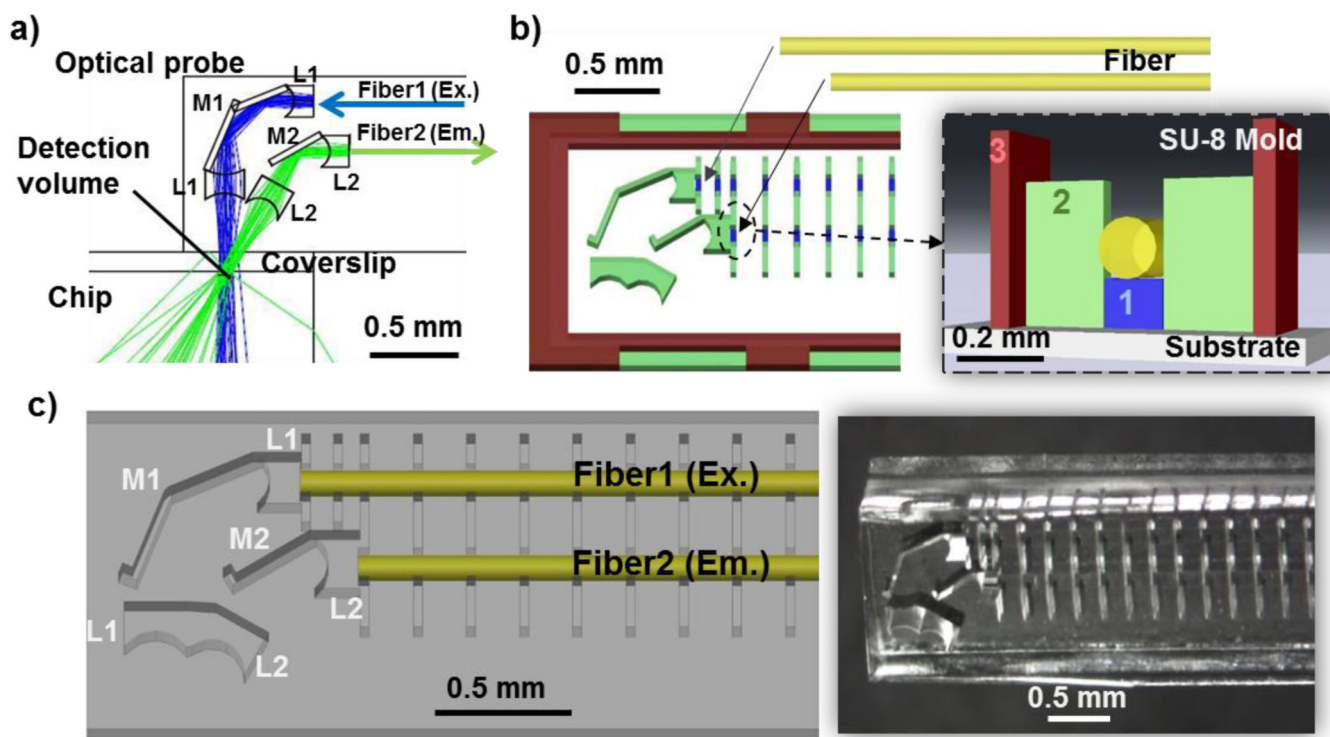
Fig. 1.
Design of a microfabricated probe. a) Zemax simulation of the optical pathway of the probe coupled to a microfluidic system. The optics include mirrors (M) and lenses (L), which are designed to focus 100 μm below the coverslip. Fiber 1 is used for guiding excitation (Ex.) light from a light source, which corresponds to 90° incidence, and Fiber 2 is used for guiding emitted light (Em.) to a detector, which corresponds to 65° incidence (° incidence= angle at which the light ray strike the sample surface. L1 and M1 reflect and focus excitation light from Fiber1 onto a sample in a microfluidic chip. L2 and M2 gather and focus the emitted light to Fiber 2. b) Drawing of a mold used to fabricate the PDMS probes. Mold is made from SU-8 photoresist on a Si substrate. The inset shows a cross-sectional view of the mold with fiber optic inserted. The mold is fabricated from 3-layers of SU-8. The drawings are color-coded by layer thickness. The blue layer (#1) is the thinnest and serves to hold the fibers at the proper height like "skids". The green layer (#2) consists of the posts for guiding and holding the fiber in place. The green layer also creates the optics on the probe tip. The red layer (#3) creates the outer boundary of the mold and therefore defines the overall probe size. Optical fibers are inserted to act as part of the mold and create a defined space for the fibers. The optical fibers are butted to the optical lenses. c) Drawing (left) and microphotograph (right) of PDMS probe created using mold in Figure 1b. The probe includes 2 optical fibers which are inserted through the guide created by the molding process. Optical components formed by air gaps (white-text label) created from the mold. The final overall probe dimensions are 1.1 mm wide × 0.52 mm thick.
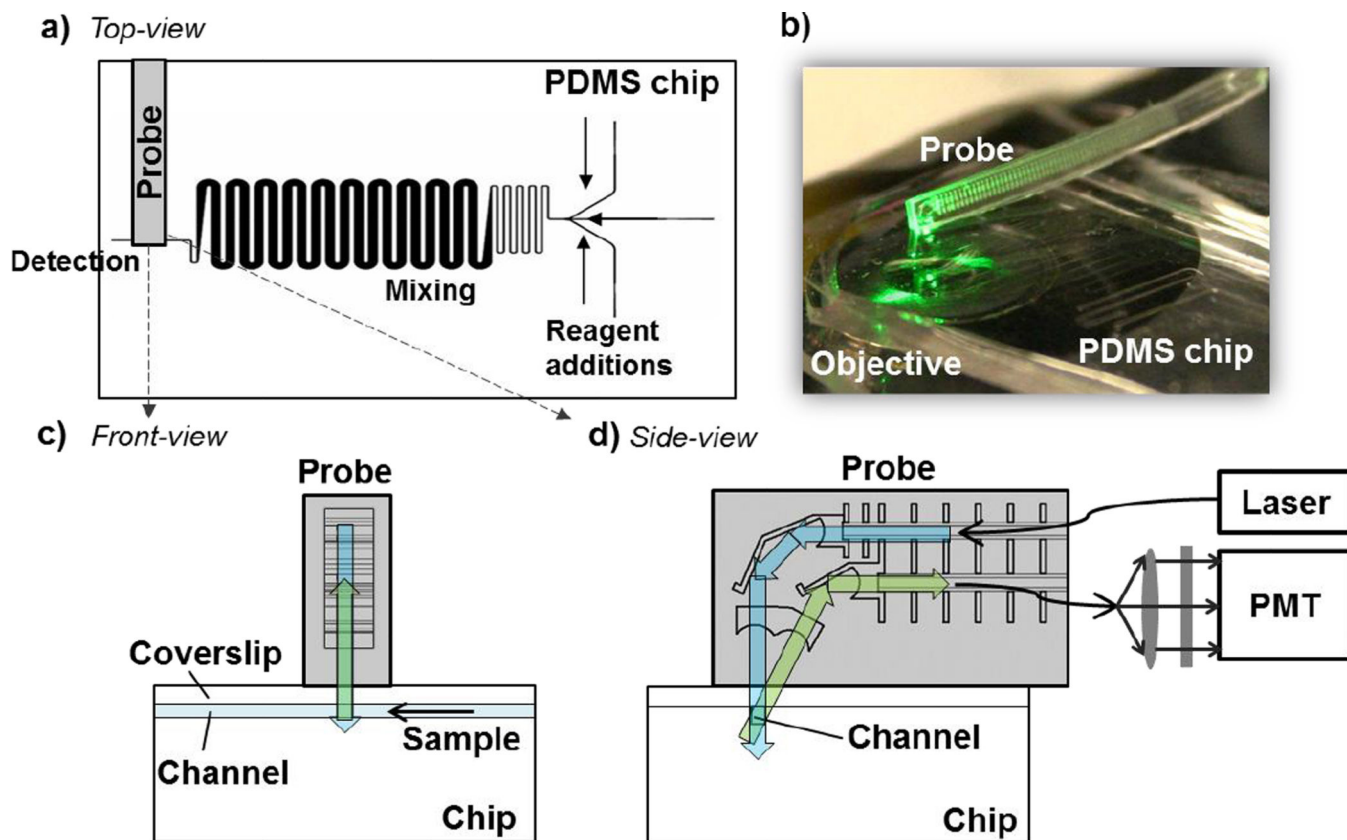
Fig. 2.
Position of probe for measuring fluorescence in microfluidic channels. a) Top-view layout of probe positioning on a PDMS-based glycerol assay chip; and b) image of the probe on the PDMS chip with comparison of probe size with a conventional microscope objective underneath the chip. c) Schematic of front-view of the probe on a chip; and d) side-view of the probe on a chip and its experimental set-up for fluorescence detection. At probe tip, the arrows indicate the light pathways into the channel (blue) and from the channel (green).
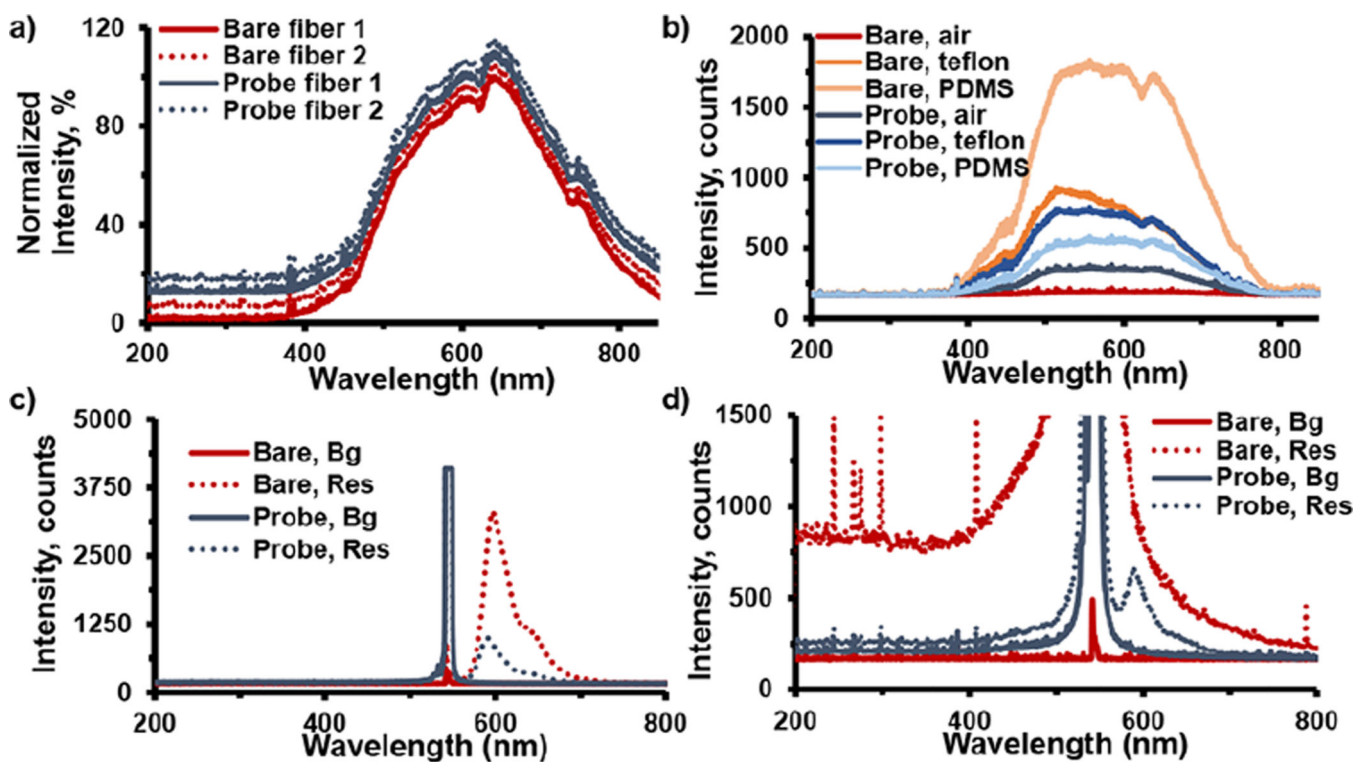
Fig. 3.

Spectroscopic performance of probe in comparison to bare fibers. a) Detection of white light through bare fibers (red) and through each lensed fiber (blue), showing identical spectral shapes. Data were offset for comparison. b) White light reflectance spectrum from varied materials. c and d) Laser excitation of 10 μM resorufin with lensed and unlensed fibers immersed in the bulk solution (c) and in microfluidic channels through a 100 μm PDMS coverslip (d). The microfabricated optics' focusing capability offset the reduced light transmission and resulted in stronger fluorescence on chip.
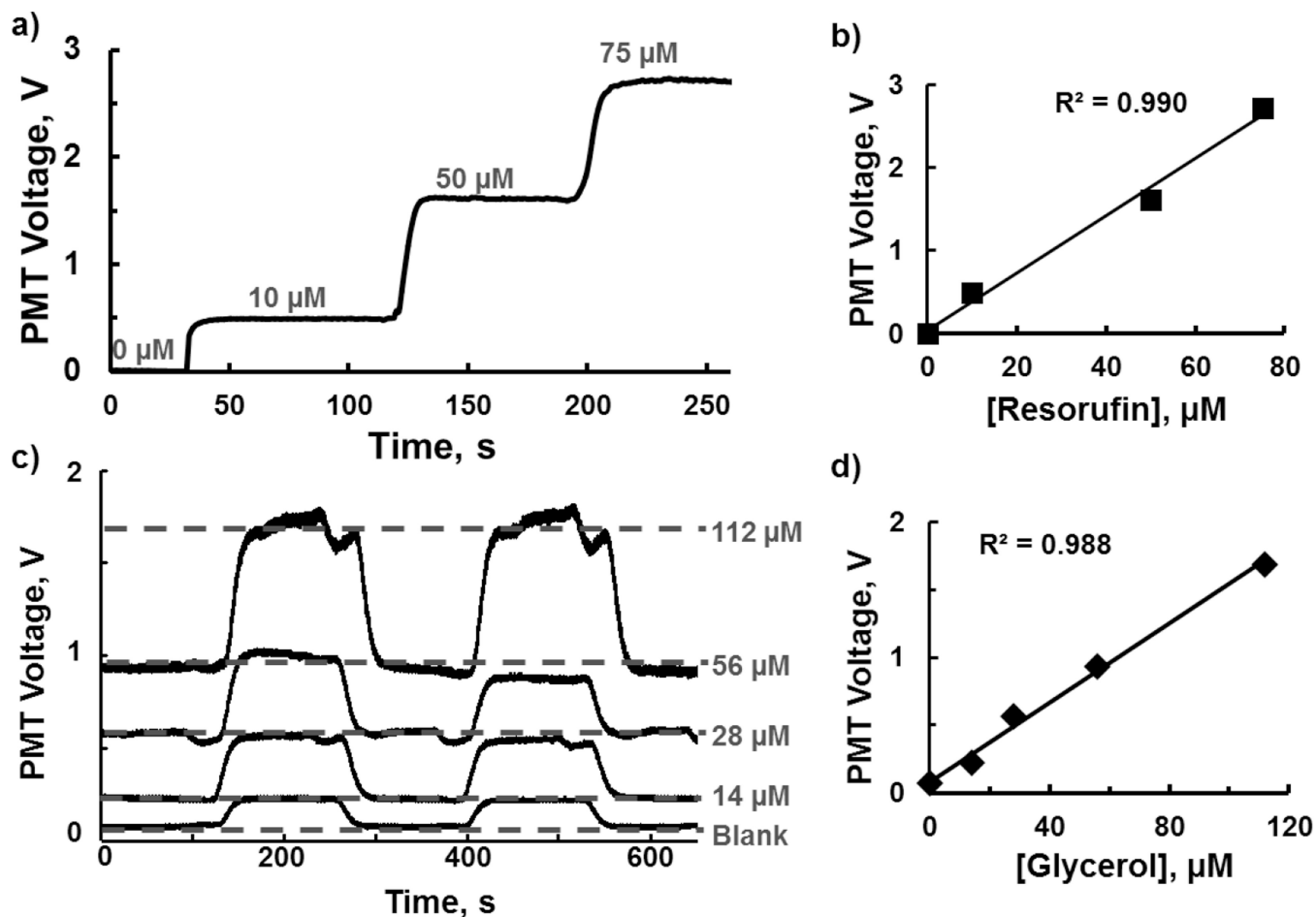
Fig. 4.
Probe performance in 60 μm deep × 100 μm wide PDMS microfluidic chips. a) Trace shows detection of fluorescence changes from 0 to 75 μM resorufin. b) Calibration curve of resorufin concentrations corresponding to (a), resulting in detection limit of 100 nM (S/N =3). c) Probe detection of on-chip glycerol assay. Individual traces show alternating between low and high glycerol concentrations (0, 14, 28, 56, 112 μM, respectively). The features at the end of each peak (prominently in 112 μM) were due to pressure switching during syringe changes. d) Linear range of glycerol assay corresponding to (c). Deviation from the line at 14 μM is inherent to the assay.
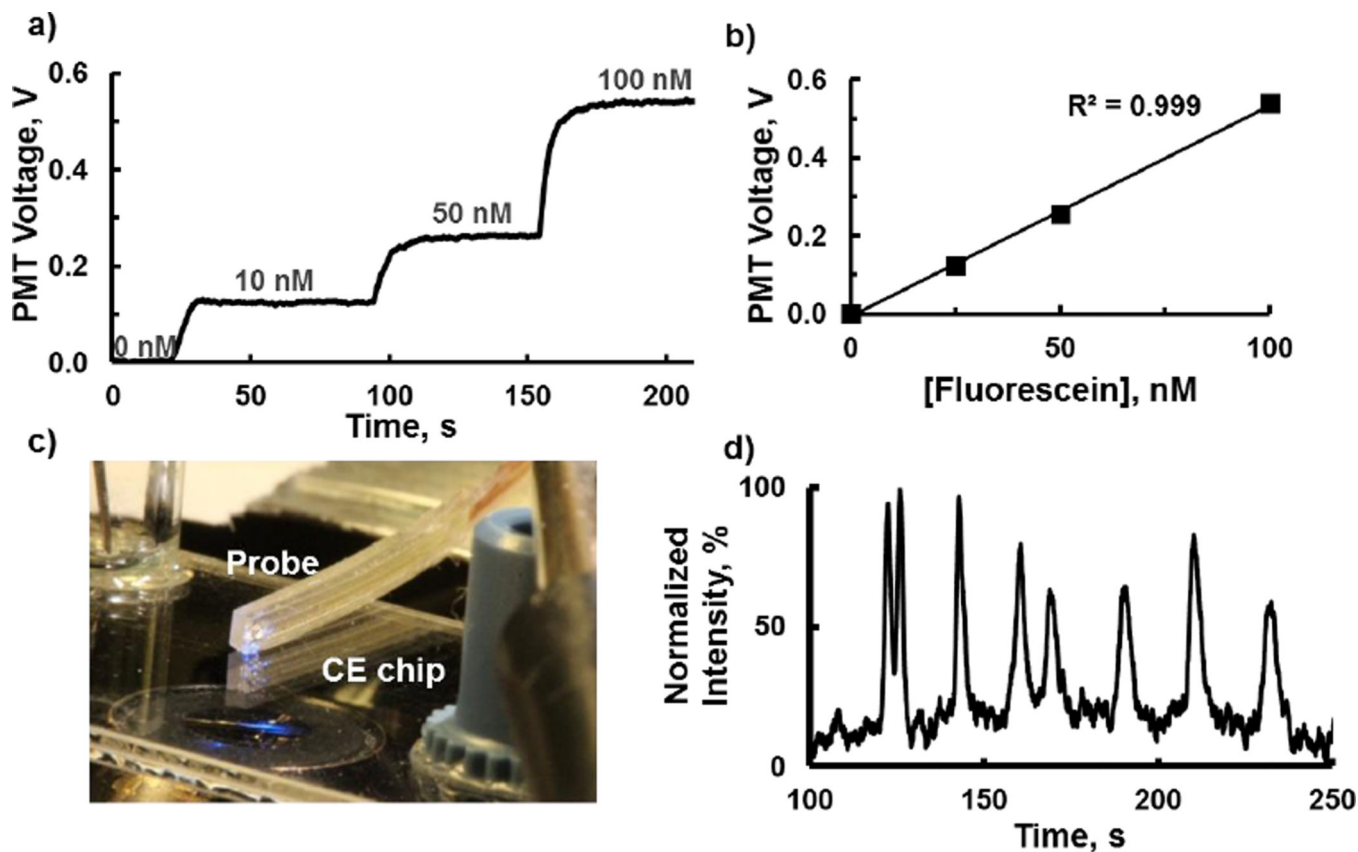
Fig. 5.
Probe performance in glass microfluidic devices. a) Trace shows detection of changes from 0 to 100 nM fluorescein in a 25 μm deep × 80 μm wide glass microfluidic channel. b) Calibration curve of fluorescein concentrations corresponding to (a), resulting in detection limit of 11 nM (S/N =3). c) Image of the probe on a glass-based electrophoresis chip, demonstrating the feasibility of using probe as a plug and play device. d) Probe detection on the electrophoresis chip of a 0.1 mg/mL protein ladder with 15 μm deep × 50 μm wide detection channel, showing electropherograms of 7 separated proteins. Doublet feature of the first protein was due to degradation of sample and/or gel, or separation conditions. These discrepancies do not influence detection.
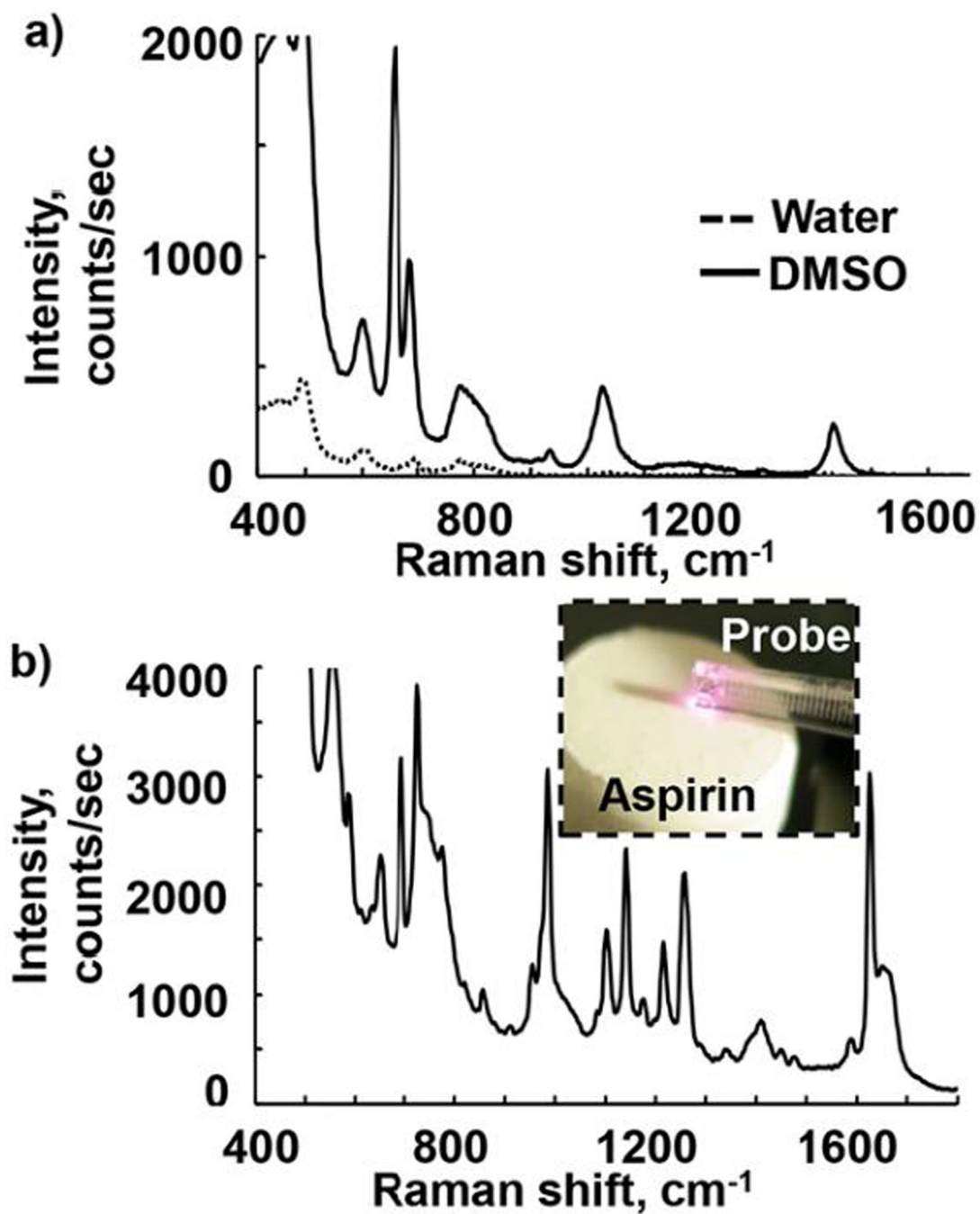
Fig. 6.
Raman spectra collected using the microfabricated probe of: a) water and DMSO as bulk solvents, and b) an aspirin tablet, as shown in the inset.